Journal Pre-proofs

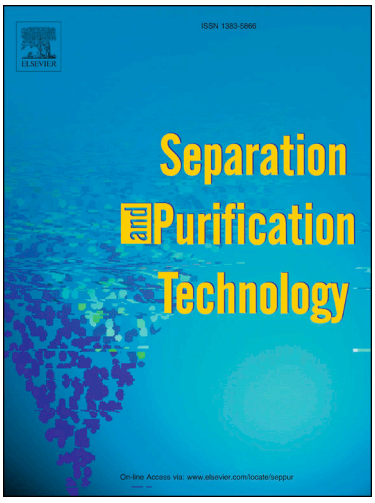

Enhanced separation of bioactive triterpenic acids with a triacontylsilyl silica gel adsorbent: from impulse and breakthrough experiments to the design of a simulated moving bed unit

Ivo S. Azenha, José P.S. Aniceto, Cristiana A. Santos, Adélio Mendes, Carlos M. Silva

PII: S1383-5866(20)31465-9
DOI: https://doi.org/10.1016/j.seppur.2020.116991
Reference: SEPPUR 116991

To appear in: *Separation and Purification Technology*

Received Date: 13 September 2019
Revised Date: 4 March 2020
Accepted Date: 4 April 2020

Please cite this article as: I.S. Azenha, J.P.S. Aniceto, C.A. Santos, A. Mendes, C.M. Silva, Enhanced separation of bioactive triterpenic acids with a triacontylsilyl silica gel adsorbent: from impulse and breakthrough experiments to the design of a simulated moving bed unit, *Separation and Purification Technology* (2020), doi: https://doi.org/10.1016/j.seppur.2020.116991

Enhanced separation of bioactive triterpenic acids with a triacontylsilyl silica gel adsorbent: from impulse and breakthrough experiments to the design of a simulated moving bed unit

Ivo S. Azenha[1], José P.S. Aniceto[1], Cristiana A. Santos[1], Adélio Mendes[2], Carlos M. Silva[1,*]

[1] CICECO, Department of Chemistry, University of Aveiro, 3810-193 Aveiro, Portugal

[2] LEPABE-Faculdade de Engenharia, Universidade do Porto, 4200-465 Porto, Portugal

*carlos.manuel@ua.pt

Keywords: biorefinery; chromatographic separation; simulated moving bed; triacontyl phases; triterpenic acids

Abstract

A simulated moving bed (SMB) unit was designed to separate oleanolic and ursolic acids, two naturally occurring triterpenoids with structural isomerism, with remarkable nutraceutical and pharmacological properties. A triacontylsilyl silica gel adsorbent (stationary phase of an Acclaim C30 column) was considered and impulse tests with different solvents were performed to select a mobile phase, from which methanol/water 95/5 (%, v/v) emerged as the most suitable. Equilibrium and global mass transport coefficients were then determined through breakthrough experiments using pure compound solutions and the C30 column. Afterwards, these parameters were applied to the simulation of two model binary mixture separations, whose breakthrough curves were also experimentally measured.

Finally, the SMB unit was designed and optimized. It was demonstrated that using the packing of an Acclaim C30 column and methanol/water 95/5 (%, v/v) as mobile phase it is possible to separate both acids with purities of 99.9 wt.%, a productivity of 1.705 kg/($m^3_{adsorbent}$ day), and a configuration of two columns per section (2-2-2-2). The simulated results obtained in this work with the C30 stationary phase represent a significant improvement over literature data.

1. Introduction

In line with the rise of the biorefinery concept and the continuous pursuit for new biosourced materials, natural products have re-emerged in the last few years since they continue to play a vital role in drug discovery [1,2]. Natural products exhibit a wide variety of pharmacophores and a high degree of stereochemistry [2], being the most successful and broadest source of chemical variability for the design of novel and effective therapeutic agents for the treatment of diseases [3].

Oleanolic (3β-hydroxyolean-12-en-28-oic) and ursolic (3β-hydroxyurs-12-en-28-oic) acids are two biologically active triterpenic acids (TTAs) that belong to one of the largest class of natural products with over 20000 identified species, the terpenoids [4,5]. These two TTAs are ubiquitous in nature and consequently integrated regularly in human diet through the consumption of several edible fruits and medicinal herbs [6–9]. Both oleanolic and ursolic acids are generally known for their anti-oxidative, antitumoral, anti-inflammatory, anti-hyperlipidemic, analgesic, hypoglycemic, anti-atherosclerotic, and anti-microbial effects [10,11]. One of the most important pharmacological properties attributed to oleanolic acid is its hepatoprotective effect against chemically induced injuries, cirrhosis and fibrosis caused by chronic liver diseases [12]. Ursolic acid, for instance, demonstrated potential as a therapeutic approach for obesity and obesity-related illness by stimulating muscle growth while simultaneously reducing fat gain [13] and also the anabolic potential to stimulate osteoblast differentiation and enhance bone regeneration [14]. Due to their wide spectrum of biological activity there has been efforts towards the incorporation of these TTAs in functional foods, cosmetics, healthcare products, drug formulations, as skin therapeutic agents, and sport supplements [15,16].

In recent years, different *Eucalyptus* species have been the object of numerous studies focusing the valorization of their residues through the production of natural extracts using organic solvents and supercritical carbon dioxide [17–22]. It is reported that the outer barks of several *Eucalyptus*

spp. possess high amounts of triterpenoids (5.2–24.6 g/kg of bark, depending on the species) [18,23,24], which are mainly triterpenic acids such as ursolic (UA) and oleanolic (OA) acids and their respective acetylated forms. In the case of dichloromethane extracts of *E. globulus bark* their occurrence may reach 5.2 g/kg, in a proportion of 55 wt.% of UA and 25 wt.% of OA. In a medium sized pulp mill using *E. globulus* wood as feedstock and producing 5×10^5 tons of bleached pulp per year, about 1×10^5 tons of bark residues are produced [25]. This points out that a new stream of high throughput and high value products can be generated from unavoidable and low value waste. These bark residues are usually burned for energy production but an intermediate extraction step could generate high-value products while still allowing most of the bark (95 – 98 wt.%) to be used for energy purposes. The separation of the triterpenic acids after extraction is, however, challenging as oleanolic and ursolic acids are structural isomers and occur simultaneously in many plants. A first step of purification can be the enrichment up till 98 % of the triterpenic acids fraction of a crude *Eucalyptus globulus* bark extract, following the procedure patented by Domingues *et al.* [26], based on a series of solvent extractions combined with pH manipulation. The presence of impurities in the final enriched stream will naturally introduce additional complexity in the subsequent purification/isolation methods, which will be reflected into the prices of the pure acids that increase greatly with increasing purity.

Different techniques such as capillary electrophoresis [27], supercritical fluid chromatography [28], thin layer chromatography (TLC) [29], gas chromatography (GC) [21,30,31], and high performance liquid chromatography (HPLC) [32–34] have been applied for qualitative and/or quantitative analysis. Amongst them, HPLC, and particularly its reversed phase mode of operation (RPLC), has been routinely used for analysis of different triterpenic acids due to its satisfactory separation efficiency and simplicity of operation. For example, in comparison with GC, it does not require any derivatization step due to the low volatility of TTAs. Regarding the column packings for the analysis of TTAs, octadecyl (C18) bonded stationary phases have doubtlessly received the most attention due to their comprehensive performance, well-studied characteristics and

commercial availability. However, while C18 bonded phases provide satisfactory results for a myriad of separations they are not ideal for all reversed phase challenges and are known to suffer from issues like partial or total loss of chromatographic retention with moderate to highly aqueous mobile phases [35] and peak broadening and tailing for basic compounds due to unfavorable interactions between solutes and residual silanols [36].

Improved separations of isomers are usually attained with longer bonded alkyl chains as the retention of nonpolar compounds becomes influenced not only by solvophobic interactions, but also from other properties of solutes such as molecular shape [37]. Triacontyl (C30) bonded phases were firstly introduced in liquid chromatography by Sander *et al*. [37,38] and since then have evolved into powerful adsorbents for the successful analysis of plant extracts, food, human tissue and synthetic mixtures containing different geometric and even optical isomers [39,40]. The longer alkyl chains increase the overall thickness of the active film of the stationary phase, promoting more extensive interactions and distribution coefficients with bigger solute molecules than the C18 alkyl chains [41,42]. Besides the remarkable high shape recognition for different type of isomers, C30 phases offer higher sample capacities making them suitable for HPLC coupled to nuclear magnetic resonance spectroscopy (HPLC-NMR) experiments where bigger samples are needed [43], and ensure more reproducible retention behavior than C18 phases when operated in highly aqueous solvent environments [41].

Simulated moving bed (SMB) chromatography is a continuous adsorption technique first patented by Universal Oil Products (UOP) [44] that has seen throughout the years an increasing number of applications devoted to fine chemistry and enantiomers separation [45–48]. SMB is an efficient alternative to batch elution chromatography as its continuous countercurrent mode of operation maximizes the mass transfer driving force, providing improved productivity, reduced solvent consumption, and complete separation of components with low chromatographic resolution [49]. Thus, an SMB process may be a potential candidate for TTAs separation. Several

works in the literature focus methodologies for the chromatographic separation/isolation of compounds by SMB [32,50–52].

In this work an SMB unit for isolating oleanolic and ursolic acids with high purity was designed using an Acclaim C30 packing material. Impulse experiments were performed to find a suitable mobile phase to conduct the separation and to determine the total and bed porosities of the column using uracil and blue dextran, respectively. Breakthrough adsorption experiments for each acid were carried out to obtain their unary isotherms and global mass transfer coefficients. The obtained parameters were then validated by assessing the prediction of breakthrough curves measured for model binary mixtures of oleanolic and ursolic acids. The triangle theory and a general optimization strategy based on a Design of Experiments – Response Surface Methodology (DoE-RSM) [53,54] were used to optimize the operating conditions (flow rates and switch times) for the SMB separation of oleanolic and ursolic acids. To our best knowledge this is the first work devoted to the comprehensive chromatographic separation of oleanolic and ursolic acids with a triacontyl (C30) stationary phase.

2. Modeling

2.1. Single column and SMB modeling

In Table 1 the chromatographic model equations along with the initial and boundary conditions are shown. Axial dispersion plug flow pattern was considered, and the internal and external mass transfer resistances were lumped into a global linear driving force coefficient. The mathematical modeling of SMB units has been addressed in several works as, for example, Hashimoto *et al.* [55], Lu and Ching [56], Pais *et al.* [57] and Aniceto and Silva [58].

Table 1 – Modeling equations of a single chromatographic column, SMB unit, and SMB to TMB equivalence.

Mass balance of component i in fluid phase of column j:	$\frac{\partial C_{ij}}{\partial t} = D_{ax,ij}\frac{\partial^2 C_{ij}}{\partial z^2} - v_j^*\frac{\partial C_{ij}}{\partial z} - \frac{1-\varepsilon_b}{\varepsilon_b}K_{LDF,ij}(q_{ij}^* - q_{ij})$	(1)
Mass balance of component i in solid phase of column j:	$\frac{\partial q_{ij}}{\partial t} = K_{LDF,ij}(q_{ij}^* - q_{ij})$	(2)
Isotherm:	$q_{ij}^* = H_i C_{ij}$	(3)
Initial conditions: (SMB and single column)	$t = 0 \;\; C_{ij}^{n=0} = 0$ or $C_{ij}^{n+1} = C_{ij}^{n}$	(4)
	$q_{ij}^{n=0} = 0$ or $q_{ij}^{n+1} = q_{ij}^{n}$	(5)
Boundary conditions (SMB):		
Column in:	$z = 0 \qquad C_{ij} - \frac{D_{ax,ij}\partial C_{ij}}{v_j^* \;\partial z} = C_{ij,0}$	(6)
Column out:		
Internal nodes:	$z = L_j \qquad C_{ij} = C_{ij+1,0}$	(7)
Eluent node:	$z = L_j \qquad C_{ij} = \frac{v_I^*}{v_{IV}^*}C_{ij+1,0}$	(8)
Feed node:	$z = L_j \qquad C_{ij} = \frac{v_{III}^*}{v_{II}^*}C_{ij+1,0} - \frac{v_F}{v_{II}^*}C_i^F$	(9)
Boundary conditions (single column):		
	$z = 0 \qquad C_i - \frac{D_{ax,i}\partial C_i}{v^* \;\partial z} = C_{i,0}$	(6)
	$z = L \qquad \frac{\partial C_i}{\partial z} = 0$	(10)
Global balances to the nodes of the SMB:		
Eluent node (E)	$v_I^* = v_{IV}^* + v_E$	(11)
Extract node (X)	$v_{II}^* = v_I^* - v_X$	(12)
Feed node (F)	$v_{III}^* = v_{II}^* + v_F$	(13)
Raffinate node (R)	$v_{IV}^* = v_{III}^* - v_R$	(14)
SMB / TMB equivalence relationships:		
Relative velocity	$v_j = v_j^* - u_s$	(15)
Switch time (t^*), solid velocity (u_s) restriction:	$u_s = \frac{L_j}{t^*}$	(16)

i – component; j – column; n – cycle number; z – axial coordinate; t – time; C_{ij} – concentration in the fluid phase; q_{ij} – average concentration in the solid phase; q_{ij}^* – solid phase concentration in equilibrium with the fluid phase; ε_b – bed porosity; $D_{ax,ij}$ – axial dispersion coefficient; $K_{LDF,ij}$ – global linear driving force (LDF) mass transfer coefficient; H_i – equilibrium constant; $v_j^* = Q_j^*/(S\varepsilon_b)$ – interstitial velocity of the fluid in the SMB; v_j – interstitial velocity of the fluid of the TMB; Q_j^* – volumetric flow rate in the SMB; S – cross section area of the column; $C_{ij,0}$ – inlet concentration of column *j*; C_i^F – feed concentration; u_s – solid velocity; t^* - switch time; L_j – column length; I, II, III, IV – section; SMB – simulated moving bed; TMB – true moving bed.

The axial dispersion coefficient of component i in a given column j ($D_{ax,ij}$) was estimated in terms of the molecular diffusion ($D_{m,i}$) and the flow around the adsorbent particles [59]:

$$D_{\mathrm{ax,ij}} = 0.73 D_{\mathrm{m,i}} + 0.5\, d_{\mathrm{p}}\, v_{\mathrm{j}}^{*} \tag{17}$$

where d_{p} is the adsorbent particle diameter and v_{j}^{*} is the interstitial fluid velocity in the SMB (or v_{j} in a single column). The molecular diffusivity was calculated by the Wilke-Chang model [60,61]:

$$D_{\mathrm{m,i}}(\mathrm{cm^2/s}) = 7.4 \times 10^{-8} \frac{T\sqrt{\phi M_{\mathrm{f}}}}{\mu_{\mathrm{f}} V_{\mathrm{bp,i}}^{0.6}} \tag{18}$$

where T is temperature (K), ϕ is a solvent dimensionless association factor, M_{f} is the solvent molecular weight (g/mol), μ_{f} is the solvent viscosity (cP), and $V_{\mathrm{bp,i}}$ is the solute molar volume at its normal boiling point (cm^3/mol). Viscosity was obtained *via* Aspen Properties® V8.4, the molar volume was calculated using the Peng-Robinson equation of state [62], and the Joback method [61,63] was adopted for the estimation of critical volume.

The SMB model equations were solved in Matlab using the method of lines. The equations were first discretized in the axial coordinate and then solved using a stiff ordinary differential equations (ODE) solver. The Nelder-Mead method was used to fit the equilibrium and mass transfer constants, minimizing the squared deviations between calculated and experimental breakthrough curves. The average absolute relative deviation ($AARD$, %) was always calculated in order to assess the goodness of fittings and predictions. For a generic function y it is given by:

$$AARD\ (\%) = \frac{100}{NDP} \sum_{i=1}^{NDP} \left| \frac{y^{\mathrm{calc}} - y^{\mathrm{exp}}}{y^{\mathrm{exp}}} \right|_{\mathrm{i}} \tag{19}$$

where superscripts calc and exp denote calculated and experimental values, and NDP is the number of data points.

2.2. SMB optimization

The Triangle Theory provides a simplified approach to SMB design by assuming instantaneous equilibrium between the solid and fluid phases (*i.e.,* mass transfer resistances are neglected) and

no axial dispersion [49,64]. Knowing the isotherm in advance, it is possible to determine a set of constrains of operating parameters (flow rates in each section of the SMB) that defines regions within which that separation is attainable. The operating parameters may be expressed as dimensionless flow rates (m_{k}) in each section k of the unit:

$$m_{\mathrm{k}} = \frac{Q_{\mathrm{k}}^{*}\ t^{*} - \varepsilon_{\mathrm{b}} V_{\mathrm{c}}}{(1-\varepsilon_{\mathrm{b}}) V_{\mathrm{c}}}, \quad k = \mathrm{I,II,III,IV} \tag{20}$$

where t^{*} is the switch time, V_{c} is the volume of each column, and Q_{k}^{*} is the internal flow rate in section k. For a feed mixture containing two components A and B, being A the most retained one, the following set of constrains defines the total separation region [46]:

$$H_{\mathrm{A}} \leq m_{\mathrm{I}} \tag{21}$$

$$H_{\mathrm{B}} \leq m_{\mathrm{II}} \leq H_{\mathrm{A}} \tag{22}$$

$$H_{\mathrm{B}} \leq m_{\mathrm{III}} \leq H_{\mathrm{A}} \tag{23}$$

$$m_{\mathrm{IV}} \leq H_{\mathrm{B}} \tag{24}$$

being section I the region between the eluent/solvent and extract nodes, section II the zone between the extract and feed nodes, section III the zone between the feed and raffinate nodes, and finally, section IV the region between raffinate and eluent/solvent nodes.

The flow rate was set to comply with the maximum pressure drop of 34 bar supported by the installation, and was calculated by the Ergun equation [65]:

$$\frac{\Delta P_{\mathrm{j}}}{L_{\mathrm{j}}} = \frac{150\ v_{0,\mathrm{j}}^{*}\ \mu_{\mathrm{f}} (1-\varepsilon_{\mathrm{b}})^{2}}{{d_{\mathrm{p}}}^{2}\quad {\varepsilon_{\mathrm{b}}}^{3}} + \frac{1.75\ \rho_{\mathrm{f}}\ {v_{0,\mathrm{j}}^{*}}^{2}}{d_{\mathrm{p}}} \left(\frac{1-\varepsilon_{\mathrm{b}}}{{\varepsilon_{\mathrm{b}}}^{3}} \right) \text{with j} = 1 \tag{25}$$

where ρ_{f} is the fluid density, and $v_{0,\mathrm{j}}^{*} = \varepsilon_{\mathrm{b}} v_{\mathrm{j}}^{*}$ is the superficial fluid velocity in the SMB.

SMB performance was evaluated using purity and productivity, two commonly used performance parameters. Purity (PuX and PuR, for extract and raffinate, respectively) is defined for both product streams and represents the ratio between the concentration of the desired component and the total concentration of all solutes:

$$PuX = 100\frac{C_{\mathrm{A}}^{\mathrm{X}}}{C_{\mathrm{A}}^{\mathrm{X}} + C_{\mathrm{B}}^{\mathrm{X}}} \; ; PuR = 100\frac{C_{\mathrm{B}}^{\mathrm{R}}}{C_{\mathrm{A}}^{\mathrm{R}} + C_{\mathrm{B}}^{\mathrm{R}}} \tag{26}$$

where A is the most retained component, B is the less retained component, and superscripts X and R denote extract and raffinate, respectively. Productivity ($Prod$) is defined as the amount of feed mixture processed per unit volume of stationary phase per unit time:

$$Prod = \frac{Q_{\mathrm{F}}\left(C_{\mathrm{A}}^{\mathrm{F}} + C_{\mathrm{B}}^{\mathrm{F}}\right)}{V_{\mathrm{T}}} \tag{27}$$

where superscript F denotes feed stream, and V_{T} is total volume of stationary phase in all SMB columns.

The determination of best operating conditions was performed by the DoE-RSM approach previously presented by the authors [54], which allows their optimization with a low number of simulations and small computational workload. Statistical software Design Expert (version 9.0, Stat-Ease, Inc.) was used for the DoE-RSM analysis and the input data were generated by the SMB simulations described in the previous section. This approach allows the determination and evaluation of direct and crossed relations between factors (independent variables) and system responses (dependent variables) over a previously defined degree of variation (levels). A small set of simulations based on model equations present in Table 1 (considering mass transfer limitations and axial dispersion) is run within the studied domain and the results are fitted to empirical models (usually polynomials) that relate the response variable Y to the factors X. In the case of second order polynomials one writes:

$$Y = \beta_0 + \sum_{\mathrm{l}=1}^{\mathrm{p}} \beta_{\mathrm{l}} X_{\mathrm{l}} + \sum_{\substack{\mathrm{l}=1 \\ \mathrm{l}\neq\mathrm{m}}}^{\mathrm{p}} \sum_{\mathrm{m}=1}^{\mathrm{p}} \beta_{\mathrm{lm}} X_{\mathrm{l}} X_{\mathrm{m}} \tag{28}$$

where β_0 is a constant, β_{l} are the coefficients of the linear effects, and β_{lm} are the coefficients of pair interactions.

In this work two factors were studied: the flow rate ratios in sections II and III of the SMB, *i.e.*, m_{II} and m_{III}. These factors were analyzed over three levels within the domain defined by the triangular separation region. The other flow rates (m_{I} and m_{IV}) were fixed as the values corresponding to the vertex of the $m_{\mathrm{I}} - m_{\mathrm{IV}}$ plane provided by the Triangle Theory. The system responses were the purities of each outlet stream and the unit productivity. The desired m_{II} and m_{III} were obtained by optimizing an embedded multi-objective function of Design Expert software, imposing a minimum purity requirement and maximizing the productivity.

It is also worth of mentioning that other optimization methods may be found in the literature like the concept of separation volume [66], the standing wave design [67], among others [68–71]. Alternatively, taking into account the equivalence between SMB and TMB, other approaches may be adopted based on the TMB analytical solutions reported initially by Hashimoto *et al*. [55] and later by Viviana *et al*. [72]. In both cases, linear isotherms and mass transfer limitations are considered except the axial dispersion contribution.

3. Experimental section

3.1. Reagents and materials

HPLC grade acetonitrile, methanol, water, and acetic acid were purchased from Sigma-Aldrich. Uracil (purity ≥ 99 %) and blue dextran with an average molecular weight of 2000000 were also purchased from Sigma-Aldrich. Oleanolic acid (purity ≥ 98 %) and ursolic acid (purity ≥ 98 %) were acquired from AK Scientific (Union City, CA). All products were used as obtained without any further purification.

3.2. High pressure liquid chromatography (HPLC) set-up

A Gilson HPLC system (Gilson, Inc., Middleton, WI, USA) equipped with a 305 isocratic controller pump, a 306 gradient pump, an 805 manometric module, an 811C dynamic mixer, and a 118 UV-vis was used to conduct the chromatographic experiments. The Gilson Unipoint Software version 5.11 (Gilson, Inc., Middleton, WI, USA) was used to record automatically all the chromatographic runs. The Acclaim C30 column (250 mm × 4.6 mm, 5 µm) column was purchased from Thermo Fisher Scientific.

3.3. Impulse experiments

A series of impulse experiments were conducted to determine column porosities (by injecting uracil and blue dextran, non-retained tracers of different molecular sizes) and to select appropriate mobile phases for the separation of oleanolic and ursolic acids. Experiments consisted of small injections of 20 µL of feed solution at room temperature (20 °C) on the Gilson HPLC system described above. UV-vis detection was set at 254 nm and 600 nm for uracil and blue dextran, respectively, and 210 nm for TTAs detection.

3.4. Unary and binary breakthrough adsorption experiments

Adsorption isotherms and global linear driving force coefficients (K_{LDF}) were determined by fitting the previously shown chromatographic model (section 2.1) to the experimental breakthrough curves. These were measured in a custom laboratorial installation as follows: after equilibrating the column with the mobile phase, a feed solution of known concentration (step signal) was continuously introduced into the column until equilibrium (adsorption stage). After that, the desorption stage was initiated switching the working pump (Knauer Azura® P 4.1S) by the mobile phase pump. Samples were collected periodically throughout the adsorption and desorption stages allowing the determination of the full breakthrough curve. The same procedure

was repeated for different feed concentrations as well as for the measurement of binary breakthrough curves.

The cumulative volume of tubing and fittings of the system (*i.e.,* extra column volume) was found to be 0.381 mL. All curves were determined at a flow rate of 1.00 mL/min and at room temperature (20 °C).

4. Results and discussion

4.1. Determination of porosities

The total porosity (ε_{T}), bed porosity (ε_{b}), and particle porosity (ε_{p}) were determined based on the elution times of two non-retained species. Total porosity was obtained using uracil, a non-retained tracer able to penetrate the particle pores, whilst the bed porosity was determined using blue dextran, which is unable to penetrate the particle pores due to its bigger size. Small injections of uracil (0.16 mg/mL in 95/5 (%, v/v) methanol/water) and blue dextran (0.76 mg/mL in 50/50 (%, v/v) methanol/water) were performed at different flow rates ranging from 0.40 to 1.40 mL/min.

The elution times (t_{r}) of non-adsorbed uracil and blue dextran were plotted against L/v_0, the ratio between column length and superficial velocity (Figure 1). Based on Eq. (29), ε_{T} and ε_{b} equal to 0.697 and 0.356, respectively, were obtained from the slopes and all coefficients of determination were above 0.999. Particle porosity (ε_{p}) was calculated from Eq. (30) and was found to be 0.530. These porosities were determined to characterize the chromatographic column packing, but only ε_{b} is necessary for column and SMB modeling.

$$t_{\mathrm{r}} = \varepsilon\frac{L}{v_0}, \text{where } \varepsilon = \varepsilon_{\mathrm{T}} \text{ or } \varepsilon_{\mathrm{b}} \tag{29}$$

$$\varepsilon_T = \varepsilon_{\mathrm{b}} + (1-\varepsilon_{\mathrm{b}})\varepsilon_{\mathrm{p}} \tag{30}$$

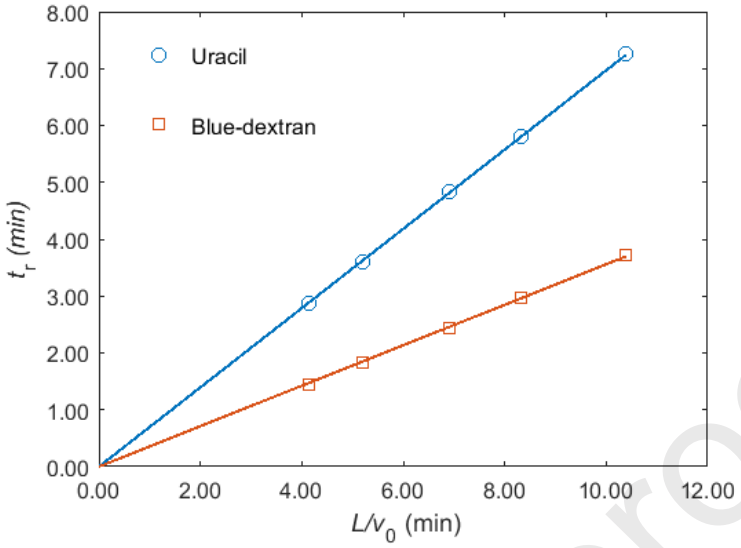

Figure 1 - Elution times of uracil and blue dextran *versus* the ratio between column length and superficial velocity for the determination of total and bed porosity, respectively. UV-vis detection at 254 nm and 600 nm for uracil and blue dextran, respectively.

4.2. Elution chromatography experiments

A series of elution experiments were performed with the Acclaim C30 column with the purpose of finding a suitable mobile phase for the separation of oleanolic and ursolic acids. It is known that the retention of oleanolic and ursolic acids is highly dependent on mobile phase composition [52,73–76], thus a careful analysis of the influence of each component in the eluent mixture is necessary to ensure that a good compromise between TTAs solubility and selectivity (and resolution) is achieved. In this work, methanol, water, acetonitrile, and mixtures thereof were used because: (i) they allow simple TTAs UV-vis detection; (ii) they do not increase significantly the pressure drop as in the case of more viscous solvents (ethanol, isopropanol, n-butanol, *etc.*), which is an important factor for scale-up; (iii) binary mixtures of methanol and water or acetonitrile increase TTAs separation ability without penalizing significantly solubility if low contents of any of those modifiers are employed [32,52].

The flow rate of the mobile phase was set to 0.40 mL/min and UV-vis detection at 210 nm. All chromatograms of this work were obtained at room temperature (20 °C) and the selectivities determined with the hold-up time of blue dextran.

The retention behavior of stationary phases is temperature-dependent, since at lower temperatures adsorption is higher and the concentration wave velocity decreases (this is very clear for linear isotherms). With relation to selectivity, very distinct trends may result: (i) Sander *et al*. [77] found that selectivity of monomeric-like C30 adsorbent towards tetrabenzonaphthalene and benzo[α]pyrene increases with increasing temperature from 5 to 50 °C; (ii) the same authors reported modest changes in selectivity over 10 – 40 °C in the case of carotenoid isomers using polymeric-like C30 column; (iii) Sánchez-Ávila *et al*. [78] reported better separation results at low temperature (optimum selectivity at 5 °C from the studied range of 5 – 35 °C) for triterpenic acids and dialcohols over a C18 stationary phase.

Regarding our experimental selectivities plotted in Figure 2, two distinct effects appear, namely, the addition of water to methanol improves the separation while the addition of acetonitrile has the opposite effect. Increasing the water content by 5 % (v/v) improves the selectivities but going beyond that has no effect on the separation. When comparing the results of methanol/water 95/5 (%, v/v) obtained with the Acclaim C30 with those reported for an Apollo C18 column [32], besides the improved separation, it is also worth to point out that both oleanolic and ursolic acids elute faster on the C30 bonded phase (*ca.* 30 %). This is in contrast with what is usually observed, for example, for the separation of different carotenoids, where C30 columns usually provide better separations but at the expense of longer analysis times [37]. However, it should be emphasized that the column packings are different, with higher total and bed porosities of 0.697 and 0.356, respectively, for the C30 column *versus* 0.623 and 0.335 for the Apollo C18. Moreover, carbon loadings are also different, with 13 and 15 % values for the C30 and C18 columns (values from the supplier), respectively. Overall, the combination of factors such as distinct alkyl chain

length (and consequently higher degree of conformational order), different carbon loading, and different architecture of the C30 phase material enables simultaneously better separations and faster analysis times.

Additionally, acetic acid 0.1 % (v/v) was introduced as an acidic modifier to the methanol and water mixtures. With methanol/water 95/5 (%, v/v) no selectivity gain was observed but with methanol/water 90/10 (%, v/v) there was in fact an improvement despite the increase of the retention times. However, this mobile phase (mainly due to the addition of acetic acid) is not attractive to run the separation of oleanolic and ursolic acids on an SMB as it penalizes the solubility of both acids. Moreover, the introduction of acetic acid poses an additional step in the preparation of mobile phase and, more importantly, another step in the recovery of solvents in a future SMB operation. For all these reasons, methanol/water 95/5 (%, v/v) (chromatogram shown in Figure 3) was the selected mobile phase to conduct further studies. All chromatograms can be found in Supplementary Material.

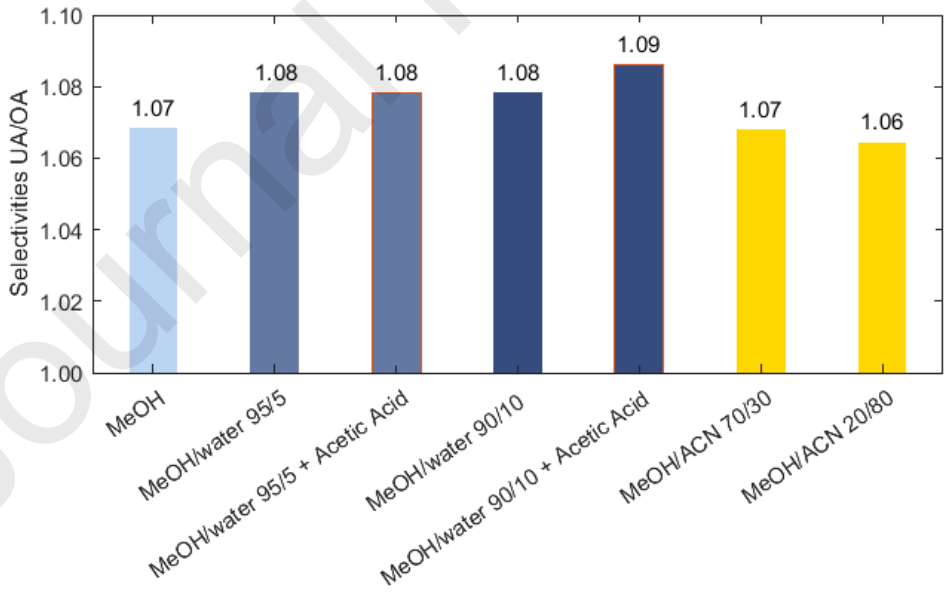

Figure 2 – Selectivities for the separation of oleanolic and ursolic acids with the Acclaim C30 column. Flow rate of 0.40 mL/min, UV-vis detection at 210 nm, 20 °C. All solvent mixture compositions are volume ratios.

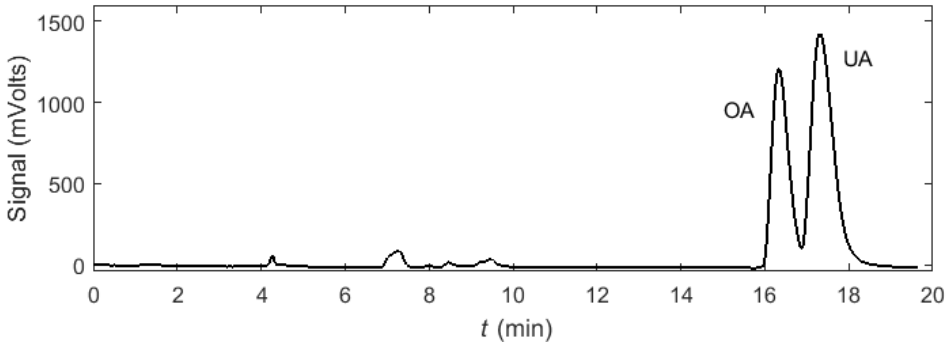

Figure 3 – HPLC chromatogram of oleanolic (OA, 0.129 mg/mL) and ursolic (UA, 0.186 mg/mL). Experimental conditions: Acclaim C30 column; mobile phase: methanol/water 95/5 (%, v/v); flow rate of 0.40 mL/min, UV-vis detection at 210 nm, 20 °C.

4.3. Unary isotherm and transport parameters determination

To determine the isotherm and global mass transfer coefficients of each compound, a series of breakthrough experiments of pure oleanolic and ursolic acids were performed in the range of 0.20 – 1.30 mg/mL and 0.20 – 2.00 mg/mL, respectively, at a flow rate of 1.00 mL/min and 20 °C. The oleanolic and ursolic experimental breakthrough curves are plotted in Figure 4 and Figure 5, respectively. The chromatographic model previously shown in section 2.1 was fitted to the experimental data by optimizing the equilibrium constant (H_{i}) and the global mass transfer coefficient (K_{LDF}), which can be found in Table 2. Overall, good results were obtained with $AARDs$ of 5.23 and 11.9 % for oleanolic and ursolic acids, respectively. The equilibrium data clearly confirmed that the isotherm trend was linear.

Additionally, the real selectivity (ratio of equilibrium constants) obtained in this work (1.09) was significantly higher than that found for a C18 packing (1.02) [32], making this column a promising candidate for the separation of these TTAs by SMB.

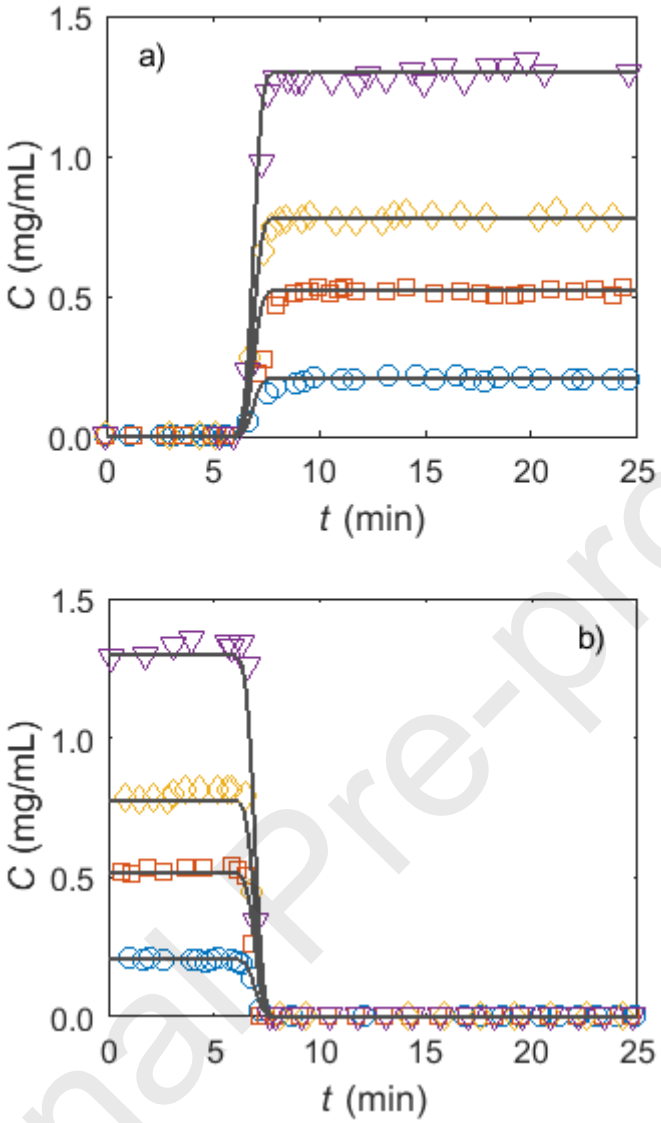

Figure 4 – Breakthrough curves of oleanolic acid with the Acclaim C30 column and 95/5 (%, v/v) methanol/water as mobile phase: a) adsorption and b) desorption stages. Symbols: ○ – 0.208 mg/mL; □ – 0.519 mg/mL; ◊ - 0.778 mg/mL; ∇ - 1.30 mg/mL. Full line: chromatographic model. Flow rate of 1.00 mL/min, UV-vis detection of 210 nm, 20 °C.

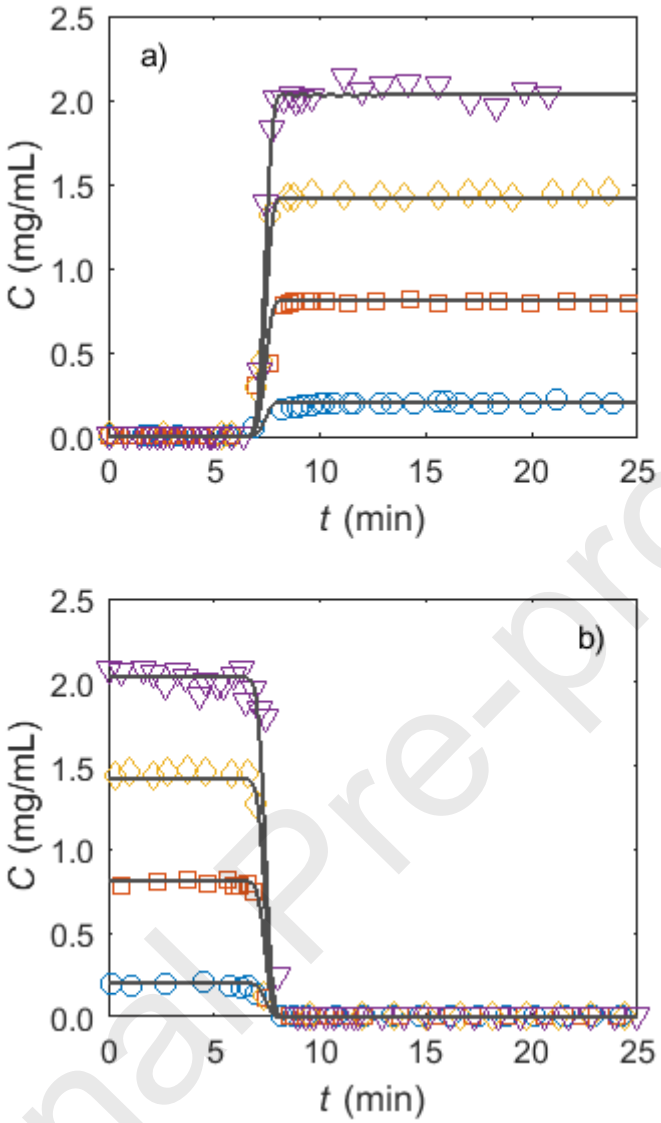

Figure 5 – Breakthrough curves of ursolic acid with the Acclaim C30 column and 95/5 (%, v/v) methanol/water as mobile phase: a) adsorption and b) desorption stages. Symbols: ○ – 0.203 mg/mL; □ – 0.812 mg/mL; ◊ - 1.42 mg/mL; ∇ - 2.03 mg/mL. Full line: chromatographic model. Flow rate of 1.00 mL/min, UV-vis detection of 210 nm, 20 °C.

Table 2 – Linear equilibrium constants and global mass transfer coefficients obtained by fitting the chromatographic model to the experimental breakthrough curves of pure oleanolic and ursolic acids. Experimental conditions: Acclaim C30 column; mobile phase: methanol/water 95/5 (%, v/v); flow rate of 1.00 mL/min, UV-vis detection at 210 nm, 20 °C.

Triterpenic Acids	Oleanolic Acid	Ursolic Acid
H	2.03	2.21
K_{LDF} (min^{-1})	112	167
D_{ax} (cm^2/min) *	4.77 × 10^{-3}	4.77 × 10^{-3}
$AARD$ (%)	5.23	11.9

* Estimated by Edwards and Richardson correlation [59].

4.4. Binary system results and modeling prediction

The parameters previously determined for the unary oleanolic and ursolic acids solutions were used to predict the two breakthrough curves of binary mixtures to assess the influence of competitive effects and to validate the use of those parameters in the SMB simulations. Two binary mixtures of oleanolic and ursolic acids with a total concentration of 0.616 and 1.232 mg/mL were fed to the column at 1.00 mL/min and 20 °C in a similar procedure as that used in the determination of pure acids breakthroughs. The ratio of oleanolic to ursolic acid was kept constant in the two runs and it was *ca.* 1:2 (wt.), respectively, to simulate a mixture from real *E. globulus* extracts [21,79]. The experimental and prediction results for the two binary mixtures are represented in Figure 6. As can be seen, the parameters determined previously for the pure acids were able to predict accurately the chromatographic separation with $AARDs$ of 5.33 and 4.78 % for the binary mixtures of 0.616 and 1.232 mg/mL, respectively, revealing the absence of competitive effects, and thus, validating the parameters to conduct SMB simulations.

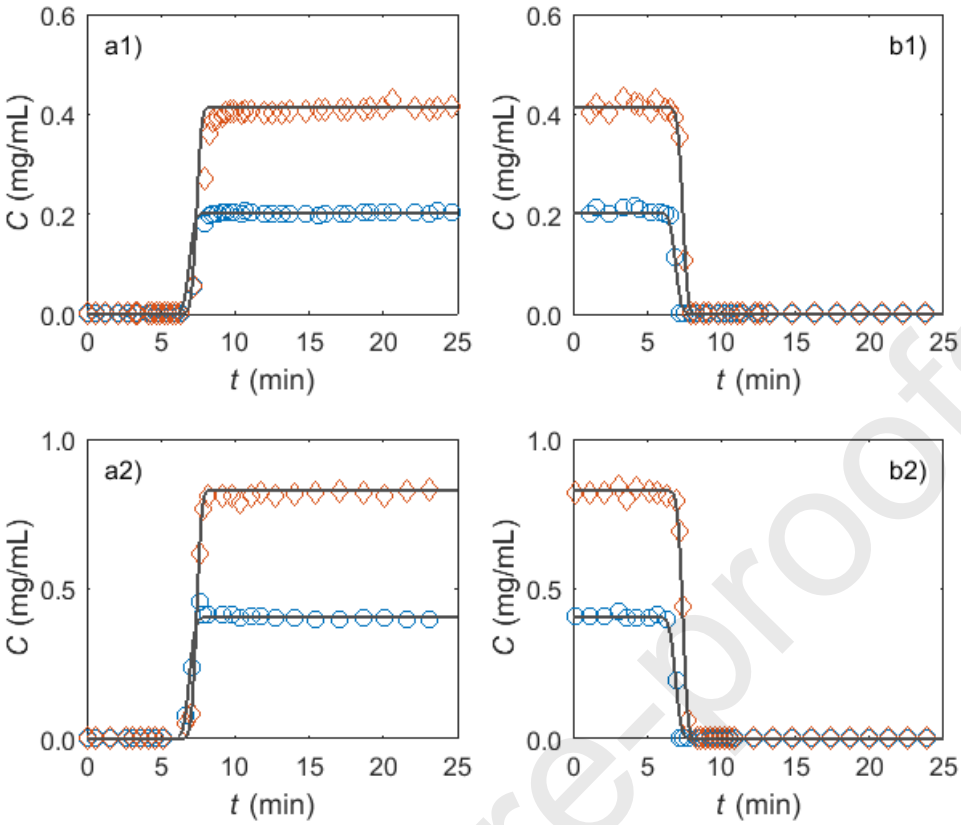

Figure 6 – Experimental and predicted breakthrough curves of binary mixtures of oleanolic (○) and ursolic (◊) acids at different feed concentrations using the Acclaim C30 column and methanol/water 95/5 (%, v/v): a1) adsorption stage with total concentration of 0.616 mg/mL and b1) desorption stage with total concentration of 0.616 mg/mL; a2) adsorption stage with total concentration of 1.232 mg/mL and b2) desorption stage with total concentration of 1.232 mg/mL. Flow rate of 1.00 mL/min, UV-vis detection of 210 nm, 20 °C. Points – experimental data; Full line – chromatographic model.

4.5. Simulation of SMB separation of oleanolic/ursolic acids mixtures

The continuous separation of oleanolic and ursolic acids by a classical SMB chromatography arrangement was studied *via* computational simulations considering, for that purpose, preparative Acclaim C30 columns.

The flow rates allowed in the SMB were estimated by considering a maximum pressure drop of 34 bar as previously discussed in section 2.2. The axial dispersion and global linear driving force coefficients (K_{LDF}) obtained for the experimental conditions of this work (from the breakthrough

assays) were then recalculated for the operating conditions of the SMB. The composition of the feed mixture was defined taking into account the following factors: (i) the mass fractions of oleanolic (25 wt.%) and ursolic (55 wt.%) acids in extracts of triterpenic acids from *Eucalyptus globulus* bark obtained by solid-liquid and supercritical fluid extraction, a process addressed by the authors [21,79]; and (ii) the solubility of oleanolic and ursolic acids in methanol/water 95/5 (%, v/v). Thus, a total concentration of 2 mg/mL was established resulting in 0.625 and 1.38 mg/mL in oleanolic and ursolic acids, respectively.

Different column lengths and SMB configurations were studied, resulting in three different scenarios: scenario 1, with a 1-1-1-1 column configuration and 25 cm length columns; scenario 2, with a 1-2-2-1 column configuration and 25 cm length columns; and scenario 3, with a 2-2-2-2 column configuration and 20 cm length columns. All data necessary for the simulations are collected in Table 3.

Table 3 - Simulation parameters for the separation of oleanolic (OA) and ursolic (UA) acids by SMB. Adsorbent: packing of Acclaim C30 column; mobile phase: methanol/water 95/5 (%, v/v); 20 °C.

	Scenario 1	Scenario 2	Scenario 3
Configuration	1-1-1-1	1-2-2-1	2-2-2-2
L_j (cm)	25	25	20
d (cm)	2.2	2.2	2.2
d_p (µm)	5	5	5
ε_b	0.356	0.356	0.356
C_{OA}^F (mg/mL)	0.625	0.625	0.625
C_{UA}^F (mg/mL)	1.38	1.38	1.38
H_{OA}	2.03	2.03	2.03
H_{UA}	2.21	2.21	2.21
$K_{LDF,OA}$ (min^{-1})	112	112	112

$K_{\mathrm{LDF,UA}}$ (min^{-1})	167	167	167
$D_{\mathrm{ax,i}}$ (cm^2/min) * Section 1	2.02×10^{-3}	1.15×10^{-3}	1.37×10^{-3}
$D_{\mathrm{ax,i}}$ (cm^2/min) * Section 2	1.92×10^{-3}	1.09×10^{-3}	1.30×10^{-3}
$D_{\mathrm{ax,i}}$ (cm^2/min) * Section 3	1.96×10^{-3}	1.12×10^{-3}	1.36×10^{-3}
$D_{\mathrm{ax,i}}$ (cm^2/min) * Section 4	1.90×10^{-3}	1.09×10^{-3}	1.30×10^{-3}
Q_1^* (mL/min)	9.41	4.70	5.88

* with three significant figures, the axial dispersion is the same for i = OA and UA.

The DoE-RSM approach [54] was then applied to optimize the separation. The optimization domain, ADE area in Figure 7, was defined to encompass the separation region provided by the Triangle Theory (ABC area) excluding points close to the diagonal as they give rise to very low productivities and thus are of little interest. A DoE grid of 13 points was created within this domain regarding the two continuous factors, *i.e.* the flow rate ratios in sections II and III of the SMB (m_{II} and m_{III}). In accordance to the response surface methodology, empirical expressions were fitted to the obtained simulated data. Quadratic models were applied to both purities while a linear model was sufficient for productivity. Upon analyzing the statistical significance of the terms of quadratic models used for both purities, these were reduced by removing the non-significant ones (those with a p-value < 0.1). The final equations are presented in Table 4. As can be seen, both coefficients of determination (R^2) and adjusted coefficients of determination (R^2_{adj}) do not differ substantially, indicating that the models do not include non-significant terms.

Table 4 – SMB responses (Extract Purity, PuX, Raffinate Purity, PuR, and productivity, $Prod$) as function of the factors m_{II} and m_{III}, and corresponding coefficients of determination (R^2) and adjusted coefficients of determination (R^2_{adj}).

Scenarios	Responses	R^2	R^2_{adj}
1	$PuX\ (\%) = -3256 + 23.68m_{\mathrm{II}} + 3047m_{\mathrm{III}} - 702m_{\mathrm{III}}^2$	0.936	0.914
	$PuR\ (\%) = -9569 + 6590m_{\mathrm{II}} + 2760m_{\mathrm{III}} - 1595m_{\mathrm{II}}^2 - 665m_{\mathrm{III}}^2$	0.950	0.925
	$Prod\ (\mathrm{kg}/(m^3\ \mathrm{day})) = -25.79m_{\mathrm{II}} + 25.79m_{\mathrm{III}}$	1.00	1.00
2	$PuX\ (\%) = -934 + 6.138m_{\mathrm{II}} + 935.4m_{\mathrm{III}} - 214.5m_{\mathrm{III}}^2$	0.968	0.957
	$PuR\ (\%) = -2790 + 2845m_{\mathrm{II}} - 21.20m_{\mathrm{III}} - 689.8m_{\mathrm{III}}^2$	0.951	0.934
	$Prod\ (\mathrm{kg}/(m^3\ \mathrm{day})) = -8.596m_{\mathrm{II}} + 8.596m_{\mathrm{III}}$	1.00	1.00
3	$PuX\ (\%) = -715.6 + 752.3m_{\mathrm{III}} - 173.4m_{\mathrm{III}}^2$	0.913	0.895
	$PuR\ (\%) = -2672 + 2676m_{\mathrm{II}} - 645.6m_{\mathrm{II}}^2$	0.913	0.896
	$Prod\ (\mathrm{kg}/(m^3\ \mathrm{day})) = -10.07m_{\mathrm{II}} + 10.07m_{\mathrm{III}}$	1.00	1.00

These reduced models were then applied to the multi-objective optimization of the oleanolic and ursolic acids separation, allowing a quick estimation of optimal operating conditions and prediction of separation performance as opposed to the time-consuming optimization routines with the numerical integration of the SMB model. For all three scenarios, a minimum purity requirement of 99 % was firstly defined for the extract and raffinate streams. This value was successively decreased by 1 % (in both streams) if the minimum purity was not attained for the

conditions provided by each scenario. The productivity was always maximized. The final complete set of optimum conditions to operate the SMB unit for each scenario, determined by conducting a few further simulations around the conditions obtained by the DoE-RSM approach to finely improve the SMB responses, are displayed in Table 5 and represented in Figure 7 by the three filled dots along with the respective separation regions.

Table 5 - Optimized operating conditions and simulation results for the SMB separation of oleanolic and ursolic acids. Adsorbent: packing of Acclaim C30 column; mobile phase: methanol/water 95/5 (%, v/v); 20 °C.

Results	Scenario 1	Scenario 2	Scenario 3
Configuration	1-1-1-1	1-2-2-1	2-2-2-2
$V_{\text{adsorbent}}$ (cm^3)	245	367	392
t^* (min)	17.98	35.97	23.02
m_{II}	2.046	2.038	2.036
m_{III}	2.117	2.118	2.205
Q_1^* (cm^3/min)	9.408	4.704	5.880
Q_2^* (cm^3/min)	8.844	4.408	5.506
Q_3^* (cm^3/min)	9.087	4.544	5.852
Q_4^* (cm^3/min)	8.788	4.394	5.493
Q_{E} (cm^3/min)	0.6198	0.3100	0.3874
Q_{F} (cm^3/min)	0.2427	0.1362	0.3603
Q_{X} (cm^3/min)	0.5644	0.2959	0.3744
Q_{R} (cm^3/min)	0.2981	0.1502	0.3733
PuX (%)	97.1	98.3	99.9
PuR (%)	97.0	98.0	99.9
$Prod$ (kg/($m^3_{\text{adsorbent}}$ day))	1.839	0.6879	1.705

E – eluent; F – feed; X – extract; R – raffinate

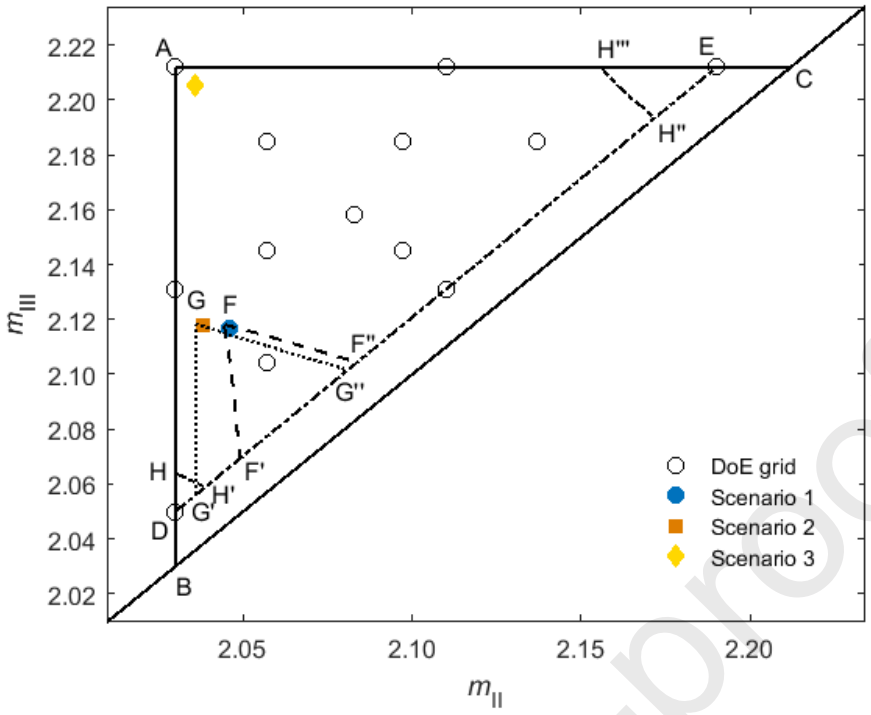

Figure 7 – Total separation region (ABCA) provided by the triangle theory, DoE domain (ADEA), simulation grid points (o), and optimized operating points for each scenario for the separation of oleanolic acid (OA) from ursolic acid (UA). The separation regions for scenario 1, scenario 2, and scenario 3 are delimited by regions (FF'F''F), (GG'G''G), and (AHH'H''H'''A), respectively. Adsorbent: packing of Acclaim C30 column; mobile phase: methanol/water 95/5 (%, v/v); 20 °C.

As can be seen in Table 5, the three different scenarios allow the separation of ursolic acid from oleanolic acid in three degrees of high purity, two of them (97 and 98 %) commonly found by TTAs vendors: (i) The one column per section configuration (1-1-1-1, scenario 1) allows the collection of oleanolic acid in the raffinate and ursolic acid in the extract with a minimum purity for both of *ca.* 97 %. The separation region (FF'F''F in Figure 7) is significantly smaller than that of the Triangle Theory (ABCA). (ii) The configuration with 2 columns in sections II and III (1-2-2-1, scenario 2) provides a minimum purity of *ca.* 98 % for both TTAs. Once again, the real separation region (GG'G''G) is smaller than the ideal one yet larger than for 1-1-1-1 arrangement. (iii) Lastly, using 2 columns per section of 20 cm (instead of 25 cm) (2-2-2-2, scenario 3), a purity of 99.9 % is obtained for oleanolic and ursolic acids with a separation region spanning almost the entire ideal area provided by the triangle theory, namely, region AHH'H''H'''A.

Regarding the different productivities, that of scenario 3 falls closely behind that of scenario 1, as the optimized operating point is closer to the vertex A (Figure 7), where the SMB productivity reaches the maximum.

With these results, it was demonstrated that an SMB unit equipped with the Acclaim C30 packing material and running with methanol/water 95/5 (%, v/v) is effectively capable of separating oleanolic and ursolic acids with purities as high as 99.9 %. This in turn represents a huge improvement over using the packing of Apollo C18 columns, for which the separation of oleanolic and ursolic acids may be accomplished with purities of 99.1 and 99.4 %, respectively, at the expense of using 3 columns per section, each column 25 cm long, resulting in very low productivities [32]. Hence, the work developed here represents an important improvement towards the effective separation of these two biologically active triterpenoids.

5. Conclusions

Oleanolic and ursolic acids are two naturally occurring triterpenic acids isomers whose molecular isolation is difficult to accomplish. Accordingly, a simulated moving bed unit was designed to perform their separation. A triacontylsilyl silica gel adsorbent, Acclaim C30 column, was selected as stationary phase and it was found that methanol/water 95/5 (%, v/v) was the most favorable solvent to conduct their continuous separation, providing a value of selectivity of 1.09. The tested C30 column demonstrated a remarkable separation capacity of these triterpenic acids due to the longer alkyl chain and consequently higher degree of conformational order, combined with different carbon loading and different column architecture and dynamics, enabling simultaneously higher selectivities and faster analysis times, when compared with previous results using an octadecyl (C18) packing material (Apollo C18) and the same mobile phase.

Afterwards, breakthrough experiments of pure acids were performed to determine isotherms and global linear driving force coefficients, which were then successfully validated in the prediction of a breakthrough of binary mixtures of oleanolic and ursolic acids. The obtained parameters were then used in the simulation of an SMB unit with a feed mixture representative from a natural extract of *E. globulus*. A classical SMB scheme was simulated and optimized using a Design of Experiments – Response Surface Methodology approach defining different purity requirements for different SMB arrangements and maximizing always the productivity.

It was demonstrated that the SMB is able to attain different purities levels of at least 97.0, 98.0 and 99.9, for both extract and raffinate outlets, and productivities of 1.839, 0.6879, and 1.705 kg/($m^3_{adsorbent}$ day) with configurations of 1-1-1-1 (25 cm columns), 1-2-2-1 (25 cm columns), and 2-2-2-2 (20 cm columns), respectively. This is a noteworthy achievement as previous results with an Apollo C18 stationary phase showed that purities of 99.4 and 99.1 % for ursolic and oleanolic acids, respectively, were achievable at the expense of using three C18 columns per section (3-3-3-3) each with a length of 25 cm, and consequently at the expense of extremely low productivities. The work presented here with the C30 column represents important improvements towards the successful chromatographic separation of these triterpenic acids.

Acknowledgements

This work was developed in the scope of the project CICECO-Aveiro Institute of Materials (FCT Ref. UID/CTM/50011/2019), financed by national funds through the FCT/MCTES and when applicable co-financed by FEDER under the PT2020 Partnership Agreement, and the Multibiorefinery project (POCI-01-0145-FEDER-016403). I.S. Azenha acknowledges a PhD grant from Fundação para Ciência e a Tecnologia (Portugal) (grant number SFRH/BD/126509/2016) and financial support of Project POCI-01-0145-FEDER-006939 (Laboratory for Process Engineering,

Environment, Biotechnology and Energy – LEPABE funded by FEDER funds through COMPETE2020 - Programa Operacional Competitividade e Internacionalização (POCI). The authors would also like to thank Mónica Válega (University of Aveiro) for the continuous support with the HPLC setup.

References

[1] F. Cherubini, The biorefinery concept: Using biomass instead of oil for producing energy and chemicals, Energy Convers. Manag. 51 (2010) 1412–1421. doi:10.1016/J.ENCONMAN.2010.01.015.

[2] A.L. Harvey, R. Edrada-Ebel, R.J. Quinn, The re-emergence of natural products for drug discovery in the genomics era, Nat. Rev. Drug Discov. 14 (2015) 111–129. doi:10.1038/nrd4510.

[3] B.B. Mishra, V.K. Tiwari, Natural products: An evolving role in future drug discovery, Eur. J. Med. Chem. 46 (2011) 4769–4807. doi:10.1016/J.EJMECH.2011.07.057.

[4] G. Wang, W. Tang, R.R. Bidigare, Terpenoids As Therapeutic Drugs and Pharmaceutical Agents, in: Nat. Prod., Humana Press, Totowa, NJ, 2005: pp. 197–227. doi:10.1007/978-1-59259-976-9_9.

[5] R.M.A. Domingues, A.R. Guerra, M. Duarte, C.S.R. Freire, C.P. Neto, C.M.S. Silva, A.J.D. Silvestre, Bioactive Triterpenic Acids: From Agroforestry Biomass Residues to Promising Therapeutic Tools, Mini. Rev. Org. Chem. 11 (2014) 382–399. doi:10.2174/1570193X113106660001.

[6] N. Kalogeropoulos, A.E. Yanni, G. Koutrotsios, M. Aloupi, Bioactive microconstituents and antioxidant properties of wild edible mushrooms from the island of Lesvos, Greece, Food Chem. Toxicol. 55 (2013) 378–385. doi:10.1016/J.FCT.2013.01.010.

[7] A. Szakiel, C. Pączkowski, F. Pensec, C. Bertsch, Fruit cuticular waxes as a source of biologically active triterpenoids., Phytochem. Rev. 11 (2012) 263–284. doi:10.1007/s11101-012-9241-9.

[8] S. Jäger, H. Trojan, T. Kopp, M. Laszczyk, A. Scheffler, S. Jäger, H. Trojan, T. Kopp, M.N. Laszczyk, A. Scheffler, Pentacyclic Triterpene Distribution in Various Plants – Rich Sources for a New Group of Multi-Potent Plant Extracts, Molecules. 14 (2009) 2016–2031. doi:10.3390/molecules14062016.

[9] Y.-C. Yang, M.-C. Wei, Ethanol solution-modified supercritical carbon dioxide extraction of triterpenic acids from *Hedyotis corymbosa* with ultrasound assistance and determination of their solubilities, Sep. Purif. Technol. 150 (2015) 204–214. doi:10.1016/J.SEPPUR.2015.06.037.

[10] D. Kashyap, H.S. Tuli, A.K. Sharma, Ursolic acid (UA): A metabolite with promising therapeutic potential, Life Sci. 146 (2016) 201–213. doi:10.1016/J.LFS.2016.01.017.

[11] J. Liu, Pharmacology of oleanolic acid and ursolic acid, J. Ethnopharmacol. 49 (1995) 57–68. doi:10.1016/0378-8741(95)90032-2.

[12] J. Pollier, A. Goossens, Oleanolic acid, Phytochemistry. 77 (2012) 10–15. doi:10.1016/j.phytochem.2011.12.022.

[13] S.D. Kunkel, C.J. Elmore, K.S. Bongers, S.M. Ebert, D.K. Fox, M.C. Dyle, S.A. Bullard, C.M. Adams, Ursolic Acid Increases Skeletal Muscle and Brown Fat and Decreases Diet-Induced Obesity, Glucose Intolerance and Fatty Liver Disease, PLoS One. 7 (2012) e39332. doi:10.1371/journal.pone.0039332.

[14] S.-U. Lee, S.-J. Park, H.B. Kwak, J. Oh, Y.K. Min, S.H. Kim, Anabolic activity of ursolic acid in bone: Stimulating osteoblast differentiation in vitro and inducing new bone formation in vivo, Pharmacol. Res. 58 (2008) 290–296. doi:10.1016/j.phrs.2008.08.008.

[15] L. López-Hortas, P. Pérez-Larrán, M.J. González-Muñoz, E. Falqué, H. Domínguez, Recent developments on the extraction and application of ursolic acid. A review, Food Res. Int. 103 (2018) 130–149. doi:10.1016/J.FOODRES.2017.10.028.

[16] C. Lin, X. Wen, H. Sun, Oleanolic acid derivatives for pharmaceutical use: a patent review, Expert Opin. Ther. Pat. 26 (2016) 643–655. doi:10.1080/13543776.2016.1182988.

[17] R.M.A. Domingues, E.L.G. Oliveira, C.S.R. Freire, R.M. Couto, P.C. Simões, C.P. Neto, A.J.D. Silvestre, C.M. Silva, Supercritical Fluid Extraction of *Eucalyptus globulus* Bark—A Promising Approach for Triterpenoid Production, Int. J. Mol. Sci. 13 (2012) 7648–7662. doi:10.3390/ijms13067648.

[18] R.M.A. Domingues, G.D.A. Sousa, C.M. Silva, C.S.R. Freire, A.J.D. Silvestre, C.P. Neto, High value triterpenic compounds from the outer barks of several *Eucalyptus* species cultivated in Brazil and in Portugal, Ind. Crops Prod. 33 (2011) 158–164. doi:10.1016/j.indcrop.2010.10.006.

[19] D.J.S. Patinha, R.M.A. Domingues, J.J. Villaverde, A.M.S. Silva, C.M. Silva, C.S.R. Freire, C.P. Neto, A.J.D. Silvestre, Lipophilic extractives from the bark of *Eucalyptus grandis x globulus*, a rich source of methyl morolate: Selective extraction with supercritical CO_2, Ind. Crops Prod. 43 (2013) 340–348. doi:10.1016/j.indcrop.2012.06.056.

[20] S.A.O. Santos, J.J. Villaverde, C.M. Silva, C.P. Neto, A.J.D. Silvestre, Supercritical fluid extraction of phenolic compounds from *Eucalyptus globulus* Labill bark, J. Supercrit. Fluids. 71 (2012) 71–79. doi:10.1016/j.supflu.2012.07.004.

[21] M.M.R. de Melo, E.L.G. Oliveira, A.J.D. Silvestre, C.M. Silva, Supercritical fluid extraction of triterpenic acids from *Eucalyptus globulus* bark, J. Supercrit. Fluids. 70 (2012) 137–145. doi:10.1016/j.supflu.2012.06.017.

[22] V.H. Rodrigues, M.M.R. de Melo, I. Portugal, C.M. Silva, Supercritical fluid extraction of *Eucalyptus globulus* leaves. Experimental and modelling studies of the influence of

operating conditions and biomass pretreatment upon yields and kinetics, Sep. Purif. Technol. 191 (2018) 173–181. doi:10.1016/J.SEPPUR.2017.09.026.

[23] C.S.R. Freire, A.J.D. Silvestre, C.P. Neto, J.A.S. Cavaleiro, Lipophilic Extractives of the Inner and Outer Barks of *Eucalyptus globulus*, Holzforschung. 56 (2002) 372–379. doi:10.1515/HF.2002.059.

[24] R.M.A. Domingues, D.J.S. Patinha, G.D.A. Sousa, J.J. Villaverde, C.M. Silva, C.S.R. Freire, A.J.D. Silvestre, C.P. Neto, *Eucalyptus* biomass residues from agro-forest and pulping industries as sources of high-value triterpenic compounds, Cellul. Chem. Technol. 45 (2011) 475–481.

[25] R.M.A. Domingues, G.D.A. Sousa, C.S.R. Freire, A.J.D. Silvestre, C.P. Neto, *Eucalyptus globulus* biomass residues from pulping industry as a source of high value triterpenic compounds, Ind. Crops Prod. 31 (2010) 65–70. doi:10.1016/j.indcrop.2009.09.002.

[26] R.M.A. Domingues, C.S.R. Freire, A.J. Silvestre, C.P. Neto, C.M.M. Silva, R.M. A. Domingues, C.S. R. F. Barros, A.J. D. Silvestre, C. P. Neto, C.M.M. Silva, Method for obtaining an extract rich in triterpenic acids from E*ucalyptus* barks, WO/2013/160881, 2013.

[27] H.-Y. Cheung, Q.-F. Zhang, Enhanced analysis of triterpenes, flavonoids and phenolic compounds in *Prunella vulgaris* L. by capillary zone electrophoresis with the addition of running buffer modifiers, J. Chromatogr. A. 1213 (2008) 231–238. doi:10.1016/j.chroma.2008.10.033.

[28] E. Lesellier, E. Destandau, C. Grigoras, L. Fougère, C. Elfakir, Fast separation of triterpenoids by supercritical fluid chromatography/evaporative light scattering detector, J. Chromatogr. A. 1268 (2012) 157–165. doi:10.1016/j.chroma.2012.09.102.

[29] M. Wójciak-Kosior, Separation and determination of closely related triterpenic acids by high performance thin-layer chromatography after iodine derivatization, 2007. doi:10.1016/j.jpba.2007.05.011.

[30] A. Guinda, M. Rada, T. Delgado, P. Gutiérrez-Adánez, J.M. Castellano, Pentacyclic Triterpenoids from Olive Fruit and Leaf, J. Agric. Food Chem. 58 (2010) 9685–9691. doi:10.1021/jf102039t.

[31] B. Martín-García, V. Verardo, L. León, R. De la Rosa, D. Arráez-Román, A. Segura-Carretero, A.M. Gómez-Caravaca, GC-QTOF-MS as valuable tool to evaluate the influence of cultivar and sample time on olive leaves triterpenic components, Food Res. Int. 115 (2019) 219–226. doi:10.1016/J.FOODRES.2018.08.085.

[32] J.P.S. Aniceto, I.S. Azenha, F.M.J. Domingues, A. Mendes, C.M. Silva, Design and optimization of a simulated moving bed unit for the separation of betulinic, oleanolic and ursolic acids mixtures: Experimental and modeling studies, Sep. Purif. Technol. 192 (2018) 401–411. doi:https://doi.org/10.1016/j.seppur.2017.10.016.

[33] S. Guo, J.-A. Duan, Y.-P. Tang, N.-Y. Yang, D.-W. Qian, S.-L. Su, E.-X. Shang, Characterization of Triterpenic Acids in Fruits of *Ziziphus* Species by HPLC-ELSD-MS, J. Agric. Food Chem. 58 (2010) 6285–6289. doi:10.1021/JF101022P.

[34] F. Gbaguidi, G. Accrombessi, M. Moudachirou, J. Quetin-Leclercq, HPLC quantification of two isomeric triterpenic acids isolated from *Mitracarpus scaber* and antimicrobial activity on *Dermatophilus congolensis*, J. Pharm. Biomed. Anal. 39 (2005) 990–995. doi:10.1016/J.JPBA.2005.05.030.

[35] X. Liu, A. Bordunov, M. Tracy, R. Slingsby, N. Avdalovic, C. Pohl, Development of a polar-embedded stationary phase with unique properties, J. Chromatogr. A. 1119 (2006) 120–127. doi:10.1016/J.CHROMA.2005.12.097.

[36] M. Zhang, W. Mai, L. Zhao, Y. Guo, H. Qiu, A polar-embedded C30 stationary phase: Preparation and evaluation, J. Chromatogr. A. 1388 (2015) 133–140. doi:10.1016/J.CHROMA.2015.02.023.

[37] L.C. Sander, K.E. Sharpless, N.E. Craft, S.A. Wise, Development of Engineered Stationary

Phases for the Separation of Carotenoid Isomers, Anal. Chem. 66 (1994) 1667–1674. doi:10.1021/ac00082a012.

[38] L.C. Sander, S.A. Wise, Effect of phase length on column selectivity for the separation of polycyclic aromatic hydrocarbons by reversed-phase liquid chromatography, Anal. Chem. 59 (1987) 2309–2313. doi:10.1021/ac00145a020.

[39] A.J. Meléndez-Martínez, M.L. Escudero-Gilete, I.M. Vicario, F.J. Heredia, Separation of structural, geometrical and optical isomers of epoxycarotenoids using triacontyl-bonded stationary phases, J. Sep. Sci. 32 (2009) 1838–1848. doi:10.1002/jssc.200800717.

[40] L.C. Sander, K.E. Sharpless, M. Pursch, C30 Stationary phases for the analysis of food by liquid chromatography, J. Chromatogr. A. 880 (2000) 189–202. doi:10.1016/S0021-9673(00)00121-7.

[41] C.A. Rimmer, L.C. Sander, S.A. Wise, Selectivity of long chain stationary phases in reversed phase liquid chromatography, Anal. Bioanal. Chem. 382 (2005) 698–707. doi:10.1007/s00216-004-2858-9.

[42] E. Turcsi, V. Nagy, J. Deli, Study on the elution order of carotenoids on endcapped C18 and C30 reverse silica stationary phases. A review of the database, J. Food Compos. Anal. 47 (2016) 101–112. doi:10.1016/J.JFCA.2016.01.005.

[43] K. Albert, Correlation between chromatographic and physicochemical properties of stationary phases in HPLC: C30 bonded reversed-phase silica, TrAC Trends Anal. Chem. 17 (1998) 648–658. doi:10.1016/S0165-9936(98)00074-0.

[44] D.B. Broughton, C.G. Gerhold, Continuous sorption process employing fixed bed of sorbent and moving inlets and outlets, US2985589A, 1961.

[45] P. Sá Gomes, M. Minceva, A.E. Rodrigues, Simulated moving bed technology: old and new, Adsorption. 12 (2006) 375–392. doi:10.1007/s10450-006-0566-9.

[46] A. Rajendran, G. Paredes, M. Mazzotti, Simulated moving bed chromatography for the separation of enantiomers, J. Chromatogr. A. 1216 (2009) 709–738. doi:10.1016/j.chroma.2008.10.075.

[47] Y. Zhang, K. Hidajat, A.K. Ray, Multi-objective optimization of simulated moving bed and Varicol processes for enantio-separation of racemic pindolol, Sep. Purif. Technol. 65 (2009) 311–321. doi:10.1016/J.SEPPUR.2008.10.050.

[48] F. Wongso, K. Hidajat, A.K. Ray, Improved performance for continuous separation of 1,1′-bi-2-naphthol racemate based on simulated moving bed technology, Sep. Purif. Technol. 46 (2005) 168–191. doi:10.1016/J.SEPPUR.2005.05.007.

[49] J.P.S. Aniceto, C.M. Silva, Simulated Moving Bed Strategies and Designs: From Established Systems to the Latest Developments, Sep. Purif. Rev. 44 (2014) 41–73. doi:10.1080/15422119.2013.851087.

[50] A. Rodrigues, C. Pereira, M. Minceva, L.S. Pais, A.M. Ribeiro, A. Ribeiro, M. Silva, N. Graça, J.C. Santos, Process Development for Liquid-Phase Simulated Moving Bed Separations: Methodology and Applications, in: Simulated Moving Bed Technology: Principles, Design and Process Applications, 1st ed., Butterworth-Heinemann, Oxford, 2015: pp. 87–115. doi:10.1016/B978-0-12-802024-1.00004-5.

[51] M. Li, Z. Bao, H. Xing, Q. Yang, Y. Yang, Q. Ren, Simulated moving bed chromatography for the separation of ethyl esters of eicosapentaenoic acid and docosahexaenoic acid under nonlinear conditions, J. Chromatogr. A. 1425 (2015) 189–197. doi:10.1016/j.chroma.2015.11.041.

[52] I.S. Azenha, J.P.S. Aniceto, S.P. Sequeira, A. Mendes, C.M. Silva, Chromatographic separation of betulinic and oleanolic acids, Sep. Purif. Technol. 235 (2020). doi:10.1016/j.seppur.2019.116129.

[53] D.C. Montgomery, Design and Analysis of Experiments, 5th Editio, John Wiley & Sons, New

York, 2000.

[54] J.P.S. Aniceto, S.P. Cardoso, C.M. Silva, General optimization strategy of simulated moving bed units through design of experiments and response surface methodologies, Comput. Chem. Eng. 90 (2016) 161–170. doi:10.1016/j.compchemeng.2016.04.028.

[55] K. Hashimoto, S. Adachi, H. Noujima, H. Maruyama, Models for the separation of glucose/fructose mixture using a simulated moving-bed adsorber., J. Chem. Eng. Japan. 16 (1983) 400–406. doi:10.1252/jcej.16.400.

[56] Z.P. Lu, C.B. Ching, Dynamics of Simulated Moving-Bed Adsorption Separation Processes, Sep. Sci. Technol. 32 (1997) 1993–2010. doi:10.1080/01496399708000750.

[57] L.S. Pais, J.M. Loureiro, A.E. Rodrigues, Modeling Strategies for Enantiomers Separation by SMB Chromatography, AIChE J. 44 (1998) 561–569. doi:10.1002/aic.690440307.

[58] J.P.S. Aniceto, C.M. Silva, Preparative Chromatography: Batch and Continuous, in: Analytical Separation Science, Wiley-VCH Verlag GmbH & Co. KGaA, Weinheim, Germany, 2015: pp. 1207–1313. doi:10.1002/9783527678129.assep047.

[59] M.F. Edwards, J.F. Richardson, Gas dispersion in packed beds, Chem. Eng. Sci. 23 (1968) 109–123. doi:10.1016/0009-2509(68)87056-3.

[60] C.R. Wilke, P. Chang, Correlation of diffusion coefficients in dilute solutions, AIChE J. 1 (1955) 264–270. doi:10.1002/aic.690010222.

[61] R.C. Reid, J.M. Prausnitz, B.E. Poling, The Properties of Gases & Liquids, 4th ed., McGraw-Hill, 1987.

[62] D.-Y. Peng, D.B. Robinson, A New Two-Constant Equation of State, Ind. Eng. Chem. Fundam. 15 (1976) 59–64. doi:10.1021/i160057a011.

[63] K.G. Joback, R.C. Reid, Estimation of pure-component properties from group-contributions, Chem. Eng. Commun. 57 (1987) 233–243.

doi:10.1080/00986448708960487.

[64] G. Storti, M. Mazzotti, M. Morbidelli, S. Carra, Robust Design of Binary Countercurrent Adsorption Separation Processes, AIChE J. 39 (1993) 471–492. doi:DOI 10.1002/aic.690390310.

[65] S. Ergun, Fluid flow through packed columns, Chem. Eng. Prog. 48 (1952) 89–94.

[66] D.C.S. Azevedo, A.E. Rodrigues, Design of a simulated moving bed in the presence of mass-transfer resistances, AIChE J. 45 (1999) 956–966. doi:10.1002/aic.690450506.

[67] Z. Ma, N.-H.L. Wang, Standing wave analysis of SMB chromatography: Linear systems, AIChE J. 43 (1997) 2488–2508. doi:10.1002/aic.690431012.

[68] Z. Zhang, K. Hidajat, A.K. Ray, M. Morbidelli, Multiobjective optimization of SMB and varicol process for chiral separation, AIChE J. 48 (2002) 2800–2816. doi:10.1002/aic.690481209.

[69] K.B. Lee, R.B. Kasat, G.B. Cox, N.-H.L. Wang, Simulated moving bed multiobjective optimization using standing wave design and genetic algorithm, AIChE J. 54 (2008) 2852–2871. doi:10.1002/aic.11604.

[70] C. Grossmann, G. Erdem, M. Morari, M. Amanullah, M. Mazzotti, M. Morbidelli, “Cycle to cycle” optimizing control of simulated moving beds, AIChE J. 54 (2008) 194–208. doi:10.1002/aic.11346.

[71] J. Bentley, C. Sloan, Y. Kawajiri, Simultaneous modeling and optimization of nonlinear simulated moving bed chromatography by the prediction-correction method, J. Chromatogr. A. 1280 (2013) 51–63. doi:10.1016/j.chroma.2013.01.026.

[72] V.M.T. Silva, M. Minceva, A.E. Rodrigues, Novel analytical solution for a simulated moving bed in the presence of mass-transfer resistance, Ind. Eng. Chem. Res. 43 (2004) 4494–4502. doi:10.1021/ie030610i.

[73] Z. Liang, Z. Jiang, D.W. Fong, Z. Zhao, Determination of Oleanolic Acid and Ursolic Acid in *Oldenlandia diffusa* and Its Substitute Using High Performance Liquid Chromatography, J. Food Drug Anal. 17 (2009) 69–77.

[74] C. Bérangère, N. Caussarieu, P. Morin, L. Morin-Allory, M. Lafosse, Rapid analysis of triterpenic acids by liquid chromatography using porous graphitic carbon and evaporative light scattering detection, J. Sep. Sci. 27 (2004) 964–970. doi:10.1002/jssc.200401764.

[75] D.I. Falev, D.S. Kosyakov, N. V. Ul'yanovskii, D. V. Ovchinnikov, Rapid simultaneous determination of pentacyclic triterpenoids by mixed-mode liquid chromatography–tandem mass spectrometry, J. Chromatogr. A. 1609 (2020) 460458. doi:10.1016/j.chroma.2019.460458.

[76] L. Olmo-García, A. Bajoub, A. Fernández-Gutiérrez, A. Carrasco-Pancorbo, Evaluating the potential of LC coupled to three alternative detection systems (ESI-IT, APCI-TOF and DAD) for the targeted determination of triterpenic acids and dialcohols in olive tissues, Talanta. 150 (2016) 355–366. doi:10.1016/j.talanta.2015.12.042.

[77] L.C. Sander, C.A. Rimmer, W.B. Wilson, Characterization of triacontyl (C-30) liquid chromatographic columns, J. Chromatogr. A. (2019). doi:10.1016/j.chroma.2019.460732.

[78] N. Sánchez-Ávila, F. Priego-Capote, J. Ruiz-Jiménez, M.D. Luque de Castro, Fast and selective determination of triterpenic compounds in olive leaves by liquid chromatography-tandem mass spectrometry with multiple reaction monitoring after microwave-assisted extraction, Talanta. 78 (2009) 40–48. doi:10.1016/j.talanta.2008.10.037.

[79] R.M.A. Domingues, M.M.R. de Melo, E.L.G. Oliveira, C.P. Neto, A.J.D. Silvestre, C.M. Silva, Optimization of the supercritical fluid extraction of triterpenic acids from *Eucalyptus globulus* bark using experimental design, 74 (2013) 105–114. doi:10.1016/j.supflu.2012.12.005.

Author Statement

Ivo S. Azenha: Writing - original draft; Investigation; Methodology

José P.S. Aniceto: Writing - original draft; Methodology; Formal analysis

Cristiana A. Santos: Investigation; Methodology

Adélio Mendes: Supervision; Writing - review & editing; Conceptualization; Formal analysis;

Carlos M. Silva: Funding acquisition; Supervision; Writing - review & editing; Conceptualization; Resources; Formal analysis

University of Aveiro, March 4th 2020

Dear Professor Bandaru Ramarao

Editor of *Separation and Purification Technology*

On behalf of all co-authors I hereby confirm that we have no conflict of interests with any researcher or entity, and that our work is being uniquely submitted to *Separation and Purification Technology.*

Carlos Manuel Silva

Chem. Eng. Group | CICECO - Aveiro Institute of Materials

Associate Professor | Department of Chemistry | University of Aveiro
Campus Universitário de Santiago
3810-193 Aveiro | Portugal

E-mail: carlos.manuel@ua.pt | Web: www,egichem.com

Phone: +351 234 401 549 | Ext: 24928

Highlights

Simulated moving bed (SMB) separation of oleanolic and ursolic acids

Several solvents and their mixtures studied for their chromatographic separation

Breakthrough assays performed to measure equilibrium & mass transfer parameters

SMB operation optimized using statistical methods and computer simulations

Both compounds isolated with purities of 99.9 % for an SMB unit of 2-2-2-2